Simulation Study of a Fixed Wireless Access System*

Nitin Gogate† Dan Avidor‡ Shivendra S. Panwar**
†Fujitsu Network Communications, Inc.
2 Blue Hill Plaza, Pearl River, NY 10965
‡Lucent Technologies, Bell Laboratories
791 Holmdel Keyport Road, Holmdel, NJ 07733
**Department of Elec. Eng., Polytechnic University
6 Metrotech Center, Brooklyn, NY 11201

1 Abstract

This paper describes a Fixed Wireless Local Loop (FWLL) system designed to provide data and voice services to fixed users. The FWLL system uses electronically steerable Base-station (BS) antennas that generate multiple narrow beams which hop around when communicating with terminals. The multiple access is provided by TDMA and the up/downlinks operate in a Frequency Division Duplex (FDD) mode. The same frequency band is reused in all the cells. With the help of simulations we evaluate the system's capacity which, in this context, is the number of serviceable terminals per cell for a given percentage of terminals that exceed a preset Signal to Interference Ratio (SIR). We also study the effect of various antenna parameters on the system's capacity. We show an improvement in capacity if a terminal has the ability to communicate with the BS to which it has the least path-loss instead of being required to always communicate with the BS located geographically closest.

2 Introduction

Advances in antenna and RF technology, microprocessors and DSP ICs have made it possible to economically build intelligent antenna systems with electronically steerable antennas that generate multiple narrow beams. We describe a FWLL system based on such an antenna subsystem which is designed to provide voice and data services to fixed users. Multiple access is provided by the TDMA technique. The uplink and downlink channels operate in Frequency Division Duplex (FDD) mode. We use a Frequency Reuse factor of 1, that is, the same frequency band is used in all the cells. Some of the cited advantages of a FWLL system include: ease of deployment, easy adaptability to new/relocated users, flexible capacity as demand grows, and low maintenance [5, 6]. FWLL can also support data rates that cannot currently be supported by the standard copper wired infrastructure.

In [9] a new metropolitan area radio system was proposed in which a BS generated a raster of narrow pencil beams, which could be rapidly scanned to any direction, to provide 360^0 coverage over a large service region. The system was shown to be well suited to emerging wide-band digital service offerings at data rates exceeding 1 Megabits/second to the end-user. The capacity of a time-space switched (TSR) cellular radio subsystem was considered in [5]. The authors investigated the performance of a sectored, cellular TSR system with multiple beams simultaneously operating in each sector. With simple propagation and interference models it was shown that the system performs very well in terms of capacity. They also demonstrated the feasibility of a frequency reuse factor of 1.

Our work differs from that presented in [5] in the following ways. This FWLL is not a sectored system, thus each beam could point anywhere in the cell. The propagation model is refined to take into account the effect of shadow fading. Further, the correlation between the shadow fading components of the path losses of links converging on a common terminal from different BSs is considered. The power control schemes, a terminal's ability to get assigned to a BS "nearest" to it in terms of path-loss as well as effects of the radiation patterns of the BS antenna are also considered.

This paper is organized as follows. In section 3 we outline the FWLL system architecture. In the following section, we present the simulation model and discuss various parameters which affect performance such as antenna radiation patterns and power control schemes. This will be followed by the methodology of evaluating the uplink and the downlink interference and SIR. We then describe a terminal assignment method which assigns a terminal to the BS to which it has the least

*The authors would like to thank Sanjay Kasturia for his support, helpful suggestions and numerous technical discussions.

0-7803-5106-1/98/$10.00 © 1998 IEEE

path-loss. Finally we conclude with discussion of results and refinements in the model which are under way.

3 System Description

The FWLL system has a number of fixed terminals and a BS at the center of every hexagonal cell. Both the terminals and the BS have directional antennas. The terminal antenna is preset to point in the direction of the BS at the time of installation. The BS antenna is electronically steerable and generates a set of narrow beams which can rotate independently in the cell. Each beam points to a terminal for a "slot" duration and then moves to face the terminal it is supposed to serve in the following time-slot. Each cell has the same number of terminals which equals the number of beams times the number of slots per frame. The structure of the BS antenna beams for a particular time slot is shown in Figure 1. During the next time slot the beams are pointing to a new set of terminals. Following the S^{th} slot the system returns to slot 1. Time is therefore segmented into a sequence of identical "frames" where each frame is a fixed sequence of "slots". Each link is supported by two beams: a downlink beam for transmission to a terminal and a uplink beam for transmission to a BS. It is not necessary that when a BS is receiving from a given terminal using slot n, it is also transmitting to the same terminal using slot n. We could, for instance, transmit to a terminal k during the n^{th} time-slot and receive from terminal k during the m^{th} time-slot. We assume that the slot-beam assignment is done at the call setup time and is not changed for the call duration. At this time we are ignoring the propagation delays, and assume that the system operates in a slot synchronous and frame synchronous mode. Hence, for this system only transmissions using time-slots in the same position in a frame interfere with each other.

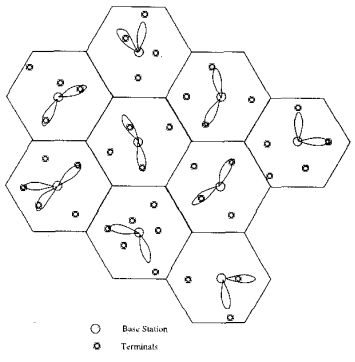

Figure 1: The service pattern for time-slot n.

As the same frequency is reused in all the cells, each link is subjected to two sources of interference, first from links within the same cell, henceforth called the intracell interference and second from all the links in the neighboring cells, henceforth called the intercell interference. As the uplinks and downlinks operate in FDD mode, they do not interfere with each other. We also assume that the system is constrained by the interference generated by transmitters belonging to the FWLL only and neglect the background noise.

4 Simulation model

We study a neighborhood of cells chosen from a continuous map of identical hexagonal cells spreading far away in all directions. When simulating the system we, by necessity, have to limit the size of the contiguous group of cells involved in the simulations. We do that by assuming that the cells, which do not belong to the group, have no transmission or reception activities inside their borders. The situation is then unbalanced because the cells on or close to the perimeter of the cluster suffer less interference than the inner cells. It is therefore clear that the cells further away from the center cell will fare better than the center cell. We can nevertheless assume that if we choose a large enough neighborhood, and apply the algorithms to the whole cluster of cells, the results of the center cell will be valid. We have chosen a group of 49 cells, shown in Figure 2, to simulate and have assumed that the interference hitting the center cell from cells outside this cluster is negligible.

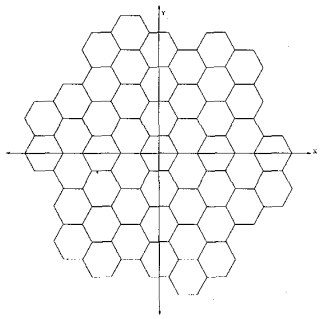

Figure 2: 49-cell cluster used in the FWLL performance evaluation.

In this model, we randomly place N terminals in every cell within the 49 cell cluster, assign a pair of time-slots to each terminal and then evaluate the percentage of terminals in the center cell with an acceptable SIR. The value for the limiting SIR should be chosen taking into consideration the fading characteristics of the signal and the interference. It seems reasonable to assume that the signal and intracell interference appear as Rician distributed signals with high K, whereas the intercell interference is Rician distributed with low K [2]. We chose the SIR threshold value to be 17 dB, since we believe that this value will provide an acceptable BER/outage time for many applications.

4.1 Antenna Radiation Pattern

For sake of reducing computation and thus reducing the simulation time, we chose to use simple antenna radiation patterns. The terminal antenna radiation pattern and one of the BS antenna patterns that we have used are shown in Figure 3. For the terminals, we approximate the radiation pattern by a rectangular pulse, the width of which is the beamwidth and it's height represents the main-beam-to-sidelobe ratio in dBs. For all the simulations we used a beamwidth of 18^o and a sidelobe level of -20 dB. For the radiation pattern of the BS antenna we used a rectangular pulse on top of a rectangular pedestal. In most simulations we used a rectangular pulse 12^o wide and 10 dBs high positioned on top of a 18^o wide and 20 dBs high pedestal (denoted as Pattern III). We compared some results with those obtained with other BS antenna radiation patterns: 8^o at -10 dB and 12^o at -30 dB; 8^o at -10 dB and 12^o at -27 dB; and 12^o at -10 dB and 18^o at -27 dB, denoted as Patterns I, II and IV respectively. Such a pattern could also be thought of as an envelope bounding from above the radiation pattern of the real antenna and having identical value at the top of the mainlobe. In this respect, the numbers presented in this work can be treated as a lower bound on performance of a system with the radiation pattern of the real antennas bounded as described above.

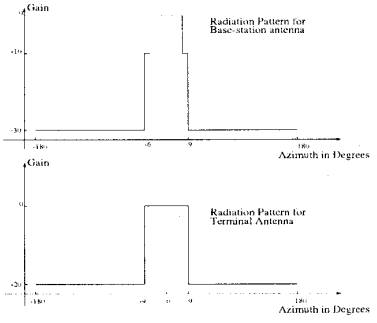

Figure 3: Antenna radiation patterns.

4.2 Propagation model

In this simulation work we have used a simple propagation model which takes into consideration distance attenuation and log-normal shadow fading [1]. Thus, the path loss associated with a link is modeled as follows,

$$[pathloss] \propto r^{-\alpha}\ 10^{\frac{\beta}{10}}, \tag{1}$$

where α is the distance attenuation coefficient, r is the distance between the transmitter and the receiver and β is the log-normal shadow fading component. Experimental data suggests the choice of 3.8 for α, a typical value for suburban areas in the 1 to 3 GHz range, and zero mean and 8 dB standard deviation for β [2, 4].

The directivity of the antennas provides additional gain/loss to the "attenuation" of the link. Taking into consideration this additional component we can write the attenuation of a link as,

$$[attenuation] \propto r^{-\alpha}\ 10^{\frac{\beta+TG+RG}{10}}, \tag{2}$$

where RG and TG are the gain of the receive and the transmit antennas in dB, respectively. We have assumed that the path-loss between a terminal and a BS is the same for the uplink and for the downlink.

4.3 Correlation Between Paths

We see the random shadowing components of the path losses of links converging on a common terminal as a set of correlated zero mean log-normal distributed random variables with a covariance matrix R given by,

$$R = \begin{bmatrix} \mu_{11} & \mu_{12} & \mu_{13} & \cdots & \mu_{1M} \\ \mu_{21} & \mu_{22} & \mu_{23} & \cdots & \mu_{2M} \\ \vdots & & \ddots & & \vdots \\ \mu_{M1} & \mu_{M2} & \mu_{M3} & \cdots & \mu_{MM} \end{bmatrix} \tag{3}$$

where μ_{ij} is,

$$\mu_{ij} = \mathrm{E}[\beta_i \beta_j], \tag{4}$$

and M is the number of cells, i.e., BSs in the simulated cluster. As said above, we have $\mu_{ii} = \sigma^2 = 8^2 = 64(\mathrm{dB}^2)$. We have assumed that links arriving at a terminal from "close" directions are highly correlated, while those arriving from significantly different bearings are only moderately correlated. At the same time, we have assumed that links converging onto a BS from different terminals are uncorrelated. The logic behind this is that the random shadow loss component of the path loss is largely determined by shadowing and obstructing objects in close proximity to the terminal antenna, which is some times located in low areas or behind buildings, and typically mounted on roof-tops or walls, while the BS antennas are typically mounted on high towers in open areas. The existence of correlation between path losses of links is mentioned in [4] in a similar scenario when computing the "other-cell interference" in a cellular CDMA system and is also discussed in [3] in the context of Macroscopic Diversity. For lack of actual field measurements, we chose to model the correlation between the shadow fading components of the path losses of link i and link j converging on a common terminal by the following formula,

$$\left.\begin{array}{lll} \mu_{ij} & = & \sigma^2(0.6999 + 0.3\ cos(\psi_{ij})), \quad i \neq j \\ & = & \sigma^2, \qquad\qquad\qquad\quad i = j \end{array}\right\} -\pi < \psi_{ij} < \pi, \tag{5}$$

where $\sigma^2 = 64\ (\mathrm{dB}^2)$ and ψ_{ij} is the angle between the two links. Notice that the maximum degree of correlation is always strictly less than 1 even for $\psi = 0$, accounting for possible separation in the vertical plane. Further, this is also a required condition for the covariance matrix to be positive definite.

Since the desired link arrives through the main lobe of the terminal antenna, we expect that the interfering paths collected by the main lobe will have their random components highly correlated with the random component of the desired path. It is easy to see that this plausible argument is likely to affect the simulation results in a "positive" way. The SIR of a typical downlink is affected directly, while the SIR of a typical uplink is affected once power control is implemented. This topic is discussed further in section 5.

4.4 Power Control

We tried out a variety of power control schemes which depend only on the link-loss and use a fixed transmit power that does not change with interference. We chose to use "full" power control for the uplink and no power control for the downlink. That is, for the uplink, the power transmitted by a terminal antenna is given by,

$$P_{\text{up}} = \frac{K_u}{r^{-\alpha}\ 10^{\frac{\beta+TG_0+RG_0}{10}}}, \tag{6}$$

where TG_0 and RG_0 are antenna transmit and receive gains in the direction of the main beam. Therefore the received power at the BS is the same for all terminals and is given by K_u Watts.

For the downlink the power transmitted by the BS antenna is fixed at K_d Watts.

The choice of the power control schemes is made on the basis of the following plausible argument. For the intracell interference, the discrimination is provided only by the BS antenna, whereas for the intercell interference, discrimination may be provided by both the BS and the terminal antennas. Thus, from the interference viewpoint, intracell interference may be quite significant for a multiple beam system. An intracell interference scenario is shown in Figure 4.

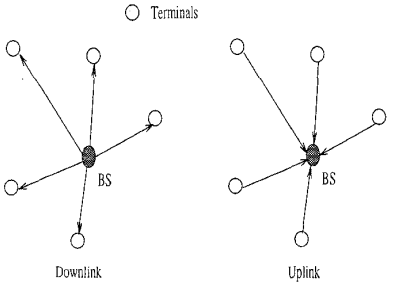

Figure 4: Intracell interference for uplink and downlink.

Assuming that there are N terminals in a cell using the same time slot then,

$$SIR^{\text{down}}_{\text{intra}} = \frac{K_d\ r^{-\alpha}\ 10^{\frac{\beta+TG_0+RG_0}{10}}}{\sum_{i=1}^{N-1} K_d\ r^{-\alpha}\ 10^{\frac{\beta+TG_0-A_{sl}+RG_0}{10}}}, \tag{7}$$

where K_d is the power radiated by the downlink BS transmitter and A_{sl} is the sidelobe suppression level of the BS antenna. Simplifying the above expression we get,

$$SIR^{\text{down}}_{\text{intra}} = \frac{1}{\sum_{i=1}^{N-1} \frac{1}{10^{A_{sl}/10}}}. \tag{8}$$

Similarly, for the uplink, the expression for SIR is,

$$SIR^{\text{up}}_{\text{intra}} = \frac{K_u}{\sum_{i}^{N-1} \frac{K_u}{r_i^{-\alpha}\ 10^{\frac{\beta_i+TG_0+RG_0}{10}}}\ r_i^{-\alpha}\ 10^{\frac{\beta_i+TG_0+RG_0-A_{sl}}{10}}}, \tag{9}$$

where K_u is the power received at the uplink BS receiver. Simplifying the above expression we get,

$$SIR^{\text{up}}_{\text{intra}} = \frac{1}{\sum_{i=1}^{N-1} \frac{1}{10^{A_{sl}/10}}}. \tag{10}$$

From equations (8) and (10) we see that, when taking only the intracell interference into account, the uplink and the downlink SIRs are equal and do not depend on the location of the terminal. The requirement for a good link is then:

$$\frac{10^{A_{sl}/10}}{N-1} > 10^{1.7}. \tag{11}$$

We can also see that all the links (up and down) have a balanced SIR for the above setup (assuming an equal load on each slot). This then leads to an equal cushion to tolerate the intercell interference.

The fact that each terminal may not need the same amount of cushion to tolerate intercell interference (specially from the downlink viewpoint) is a motivation to look into other power control schemes, but we have not explored this subject further.

5 Interference Evaluation

We place N terminals using uniform probability distribution over the area of each cell. These terminals are served by a set of (B) hopping beams. Thus the maximum number of intracell interferers is $B-1$ and the maximum number of interferers located in any other cell is B. So, for our system with 49 cell cluster, there are a maximum of $48B$ intercell interferers.

For the downlink, the BS radiates constant power preset to K_d Watts and there is no power control. The SIR for a downlink j is given by,

$$SIR^{\text{down}}_{j} = \frac{K_d\ r_j^{-\alpha}\ 10^{\frac{\beta_j+TG_0+RG_0}{10}}}{\sum_i K_d\ (r^d_{ji})^{-\alpha}\ 10^{\frac{\beta_{ji}+TG^d_{ji}+RG^d_{ji}}{10}}}, \tag{12}$$

or,

$$SIR^{\text{down}}_{j} = \frac{1}{\sum_i (\frac{r^d_{ji}}{r_j})^{-\alpha}\ 10^{\frac{\beta_{ji}-\beta_j+TG^d_{ji}-TG_0+RG^d_{ji}-RG_0}{10}}}, \tag{13}$$

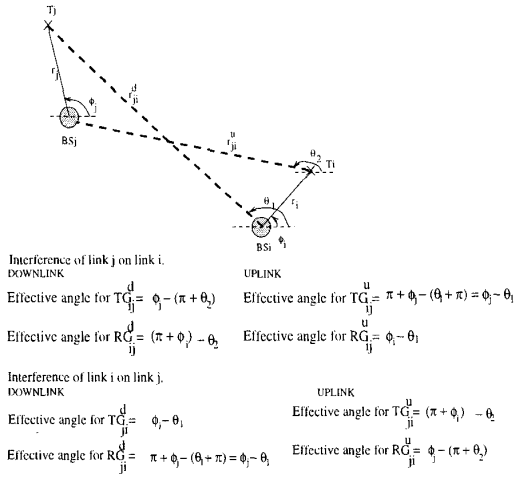

Figure 5: Interference Evaluation of two links in two different cells.

where the summation is over all possible interferers (i.e., all the BSs and beams using the same slot-position). As described earlier, the log-normal shadowing components β_{ji} and β_j are correlated with a degree of correlation dependent on the angle (ψ) between the two links which converge on this common terminal. r_j is the distance of terminal j from its BS and r^d_{ji} is the distance between the desired terminal receiver and the i^{th} interfering BS transmitter. TG^d_{ji} and RG^d_{ji} are antenna gains in the appropriate azimuths as shown in Figure 5.

Proceeding along similar lines, for the uplink which is fully power controlled (i.e. power control compensates for the full path loss including log-normal shadowing component), the power received at a desired receiver is K_u Watts. The power transmitted by the i^{th} interfering transmitter is

$$\frac{K_u}{r_i^{-\alpha}\ 10^{\frac{\beta_i + TG_0 + RG_0}{10}}}. \tag{14}$$

The SIR for an uplink j is given by,

$$SIR_j^{\text{up}} = \frac{K_u}{\sum_i \frac{K_u}{r_i^{-\alpha}\ 10^{\frac{\beta_i + TG_0 + RG_0}{10}}} (r^u_{ji})^{-\alpha}\ 10^{\frac{\beta_{ij} + TG^u_{ji} + RG^u_{ji}}{10}}}, \tag{15}$$

or,

$$SIR_j^{\text{up}} = \frac{1}{\sum_i (\frac{r^u_{ji}}{r_i})^{-\alpha}\ 10^{\frac{\beta_{ij} - \beta_i + TG^u_{ji} - TG_0 + RG^u_{ji} - RG_0}{10}}}. \tag{16}$$

Note that TG^d_{ji} is equal to RG^u_{ij} and similarly TG^u_{ji} is equal to RG^d_{ij}. Looking at Figure 5 and equations (13) and (16), it is then clear that the interference contribution of the downlink BS transmitter i at terminal receiver j is the same as that of the uplink terminal transmitter j at the BS receiver i. That is, the two cases are symmetric. From equations (13) and (16), it is also evident that the correlation between the shadow losses of links converging on a common terminal affect the system performance (both downlink and uplink) favorably: $\mathrm{E}\left[10^{\frac{\beta_{ij} - \beta_i}{10}}\right]$ is smaller when β_{ij} tends to track β_i (where $\mathrm{E}[\cdot]$ denotes the expected value).

6 Slot-beam Assignment

The performance of the system depends heavily on the choice of the "slot assignment algorithm". The simplest algorithm might assign the first terminal in each cell to the first slot of the first beam, the second to the second slot of the first beam and then, when all the slots of the first beam are occupied, to the first slot of the second beam and so forth. Pairs or larger sets of terminals served by overlapping beams during the same slot will experience high level of mutual interference, and neither of them will reach the minimal SIR threshold. Further degradation is caused by transmitters located in neighboring cells. We could employ an intelligent slot assignment algorithm which takes advantage of the known positions of all active terminals over a large enough area to minimize the mutual interference between beams during each slot. An optimal algorithm to do this kind of "coordination" is probably too complicated to be of practical use. We have, in this work, chosen the following algorithm which considers only the intracell interference while making assignments.

The BS in each cell attempts to assign slot-beam pairs sequentially. For every assignment, a BS starts by scanning the first beam for an empty slot and checks if it can be used. The usability criterion is that the slot-beam combination must satisfy two requirements:
a) It would not adversely affect (violate the SIR constraint) any other assignment that has already been made in that same cell.
b) The combined effect of all other links in that same cell using the same slot on this "possible" allocation does not violate its SIR constraint.
If the slot cannot be used it will try the next empty slot in the same beam. After all empty slots in a beam have been checked, the next beam is scanned. If no usable slot-beam pair can be found for a terminal, it is rejected and will not be serviced.

7 Terminal Assignment to the "Best" BS

In the first part of this study we assumed that the terminals are assigned to the BS in the center of their cell, i.e., to the geographically nearest BS. We also present results for a case in which the terminals are assigned to a BS to which it has the minimum path-loss. A terminal

j gets assigned to a BS k for which,

$$r_{jk}^{-\alpha} 10^{\frac{\beta_{jk}}{10}} \geq r_{ji}^{-\alpha} 10^{\frac{\beta_{ji}}{10}} \quad \text{for every} \quad i \neq k. \qquad (17)$$

8 Simulation Procedures and Results

The method for evaluating the FWLL performance is as follows.

Comment: Frame size (S) = 10 slots, number of beams (B) serves as the independent parameter.

1. Let m (number of iterations) = 0.
2. Place $N = B * S$ terminals randomly in each cell.
3. For each terminal in every cell, compute the shadow loss covariance matrix and accordingly select the random shadowing component of the path losses of all the links converging on that terminal.
4. Calculate the total path loss and the Transmit power for every Terminal-BS pair.
5. For each terminal in every cell, perform the slot-beam allocation using the algorithm described in section 6.
6. For all the terminals in the center cell, calculate the uplink and the downlink SIRs, considering both the intracell and the intercell interference. Count the number of bad connections, i.e., connections with either uplink or downlink SIR < 17 dB. Those terminals which cannot be allocated a slot-beam pair are also counted as bad connections.
7. Increment m.
8. If (m < 1000) Go back to 2 else, sum up the number of bad connections from all iterations and calculate the percentage of terminals with bad connections.

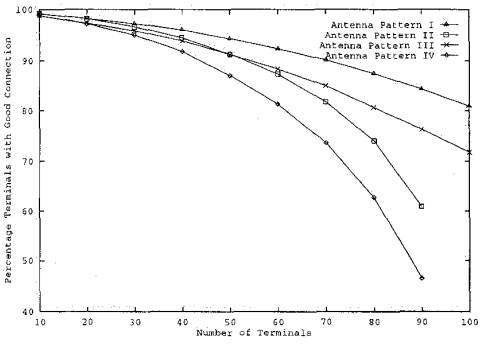

Figure 6: Percentage of users with good connection as a function of the total number of users, Num. of slots/frame (S): 10 and Num. of Term./cell (N): 10*B.

The effect of the beam width and the sidelobe suppression level of the BS antenna on capacity is shown in Figure 6 which compares the system capacity for various sets of parameters. As expected, we observe that the capacity is lower when we use BS antenna with either wider mainlobe or lower sidelobe suppression level. Comparing the results for Antenna Patterns II and III, we observe that for a lightly loaded system, that is, with low number of interferers, antenna II which has narrower mainlobe, performs better than antenna III, even though, it has worse sidelobe suppression level. For uplink (downlink) this may be due to the fact that for lightly loaded systems the interference captured by (radiated through) the main lobe dominates, whereas as the system becomes heavily loaded, that is, a higher number of interferers, interference captured by (radiated through) the sidelobes dominates. In designing a BS antenna, there is usually a trade-off between mainlobe width and sidelobe suppression level. Figure 6 may guide the designer in making such a trade-off.

Another way of representing the above results is by plotting the average number of good connections that can be supported on a time-slot as a function of the number of beams. This is shown in Figure 7. We see that, in general, the average number of good connections supported per time-slot initially increases, then tends to saturate and then falls. This is due to increased level of intercell interference. This behavior can be seen in Figure 7 from the plots for antenna patterns with lower sidelobe suppression.

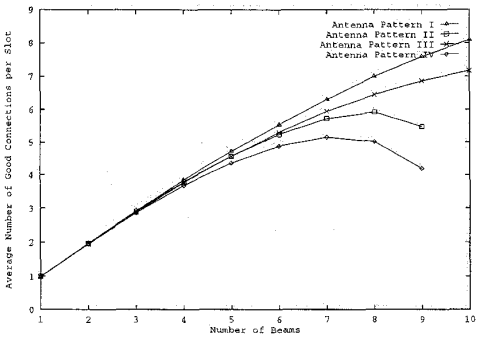

Figure 7: Average number of good connections per time-slot as a function of the number of beams for the case S=10, N=10*B.

As described in section 4.3 correlation between the shadow fading components of the path losses of the links converging on a common terminal affects the performance in a significant way. The effect of the degree of correlation on the percentage of terminals with good connection is shown in Figure 8. For the 5% bad connections criterion, we see a loss of capacity by almost 28.8 %, if we reduce the parameter α from 0.6999 to 0.6. As we further reduce the degree of correlation we further lose capacity. If the random shadow losses are modeled as uncorrelated random variables, then the performance is the worst and percentage of bad connections is greater than 5% even with one beam.

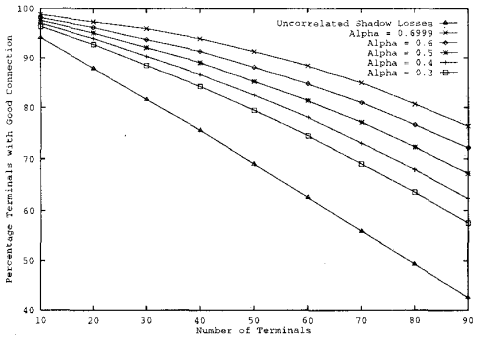

Figure 8: Percentage of users with good connection versus Degree of Correlation between the shadow-losses for the case S=10, N=10*B and BS with antenna pattern III.

8.1 Results of Terminal Assignment to the "Best" BS

The simulation methodology is described below. We start by placing a large number of terminals uniformly over the cell area in every cell. Following the link-loss calculation, we assign the terminals to the BSs they have the least path-loss to. Thus, after such an assignment, every BS will in general have a different number of terminals to support. To compare the results with the previous case in which terminals are assigned to the geographically closest BS, we randomly remove the extra number of terminals from each cell, such that all the cells have exactly same number of terminals. That is, there is one terminal per beam per slot.

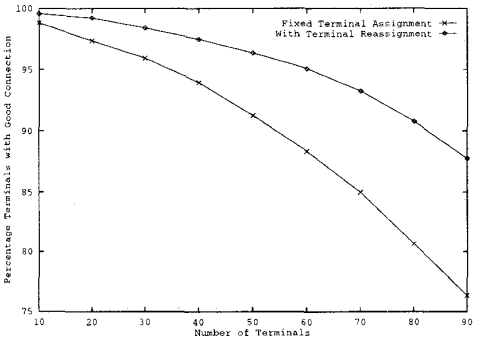

Figure 9: Effect of terminal assignment to the "best" BS on percentage of users with good connection for the case S=10, N=10*B and BS with antenna pattern III.

Broadly speaking, terminal assignment to the "best" BS serves the following two purposes. For the uplink we now radiate less power, hence cause less interference to other links which leads to higher SIR. Whereas for the downlink, the average SIRs at the intended receivers is now increased directly. The results are plotted in Figure 9. We see that for the 5% bad connections criterion, the number of terminals that can be supported improves by almost 74.2%.

9 Conclusion

We have presented a TDM based FWLL system to provide voice and data services to fixed users. With the help of simulations, we showed that even with a simple slot-beam assignment algorithm, which takes into account intracell interference only, a good capacity is achieved. The system performance is shown to be critically dependent on the side-lobe suppression level and the beam width of the BS antenna. It is also shown that correlation between the random shadow fading component of the path losses of links converging on a common terminal affects the system performance in a major way. To the best of our knowledge, field measurements and data which can be used to establish a reliable correlation model, as discussed above, are not available in open literature and is a subject for investigation. As expected, the performance is further improved by assigning the terminals to the BSs to which they have minimum path loss. There is no doubt that the performance can be significantly improved by coordinating the slot-beam assignments with neighboring cells. In a dynamic situation, such coordination is quite complicated, though, and will consume back-bone network resources.

References

[1] W.C.Y. Lee, Mobile Cellular Telecommunication Systems, McGraw-Hill Book Company, 1989.

[2] R. Steele, Mobile Radio Communications, Pentech Press, 1992.

[3] H. W. Arnold, D. C. Cox and R. R. Murray, "Macroscopic Diversity Performance Measured in the 800 MHz Portable Radio Communications Environment," *IEEE Tran. on Comm.*, Vol. 36, No. 2, February 1988.

[4] A. J. Viterbi, A. M. Viterbi and E. Zehavi, "Other-Cell Interference in Cellular Power-Controlled CDMA," *IEEE Tran. on Comm.*, pp. 1501-1504, Vol. 42, No. 2/3/4, February/March/April 1994.

[5] J. Zander and K. Ahl, "On the Capacity of Time-Space Switched Cellular Radio Link Systems for Metropolitan Area Networks," *Proc. of the IEE*, pp. 533-538, Vol. 139, No. 5, October 1992.

[6] D. L. Jones, "Fixed Wireless Access: A Cost Effective Solution for Local Loop Service in Underserved Areas," *Proc. of ICWC*, pp. 240-244, 1992.

[7] A. R. Lopez, "Performance Predictions for Cellular Switched-Beam Intelligent Antenna Systems," *IEEE Comm. Mag.*, pp. 152-154, October 1996.

[8] V. K. Garg and E. L. Sneed, "Digital Wireless Local Loop System," *IEEE Comm. Mag.*, pp. 112-115, October 1996.

[9] A. Acampora, T. Chu, C. Dragone, and M. Gans, "A Metropolitan Area Radio System Using Scanning Pencil Beams," *IEEE Tran. on Comm.*, pp. 141-151, Vol. 39, No. 1, January 1991.